

***J*-Spectroscopy in the presence of residual dipolar couplings: determination of one-bond coupling constants and scalable resolution**

Julien Furrer · Michael John · Horst Kessler ·
Burkhard Luy

Received: 17 November 2006 / Accepted: 29 November 2006 / Published online: 19 January 2007
© Springer Science+Business Media B.V. 2007

Abstract The access to weak alignment media has fuelled the development of methods for efficiently and accurately measuring residual dipolar couplings (RDCs) in NMR-spectroscopy. Among the wealth of approaches for determining one-bond scalar and RDC constants only *J*-modulated and *J*-evolved techniques retain maximum resolution in the presence of differential relaxation. In this article, a number of *J*-evolved experiments are examined with respect to the achievable minimum linewidth in the *J*-dimension, using the peptide PA₄ and the 80-amino-acid-protein Saposin C as model systems. With the JE-N-BIRD^{d,X}-HSQC experiment, the average full-width at half height could be reduced to approximately 5 Hz for the protein, which allows the additional resolution of otherwise unresolved peaks by the active (*J*+*D*)-coupling. Since RDCs generally can be scaled by the choice of alignment medium and alignment strength, the technique introduced here provides an effective resort in cases when chemical shift differences alone are insufficient for discriminating signals. In favorable cases even secondary structure elements can be distinguished.

Keywords RDCs · BIRD-element · Scalable resolution · *J*-Evolution · *J*-Spectroscopy

Introduction

Although media for very weak alignment are known for only a relatively short period (Tjandra and Bax 1997a; Hansen et al. 1998; Prestegard 1998; Bendiak 2002; Freudenberger et al. 2004, 2005; Luy et al. 2004; Habertz et al. 2005), residual dipolar couplings (RDCs) have already become a standard structural parameter in NMR spectroscopy of biomolecules (Simon and Sattler 2002; Bax 2003), and are also becoming more and more popular for organic molecules (Martin-Pastor and Bush 2001; Freedberg 2002; Thiele and Berger 2003; Verdier et al. 2003; Yan et al. 2003, 2004; Klages et al. 2005). The interest in methods for rapid and accurate determination of heteronuclear and homonuclear coupling constants has brought up a wealth of techniques (e.g., Tolman and Prestegard 1996b; Tjandra and Bax 1997b; Brutscher et al. 1998; Ottiger et al. 1998b; Yang et al. 1998). Most approaches designed for the determination of most easily accessible one-bond heteronuclear coupling constants rely on the measurement of the displacement between doublet components in *J*-coupled spectra with (Meissner et al. 1997a, b; Brutscher et al. 1998; Ottiger et al. 1998a; Luy et al. 2001; Permi 2002) or without spin state selective elements (Tolman and Prestegard 1996a; Bax and Tjandra 1997; Tjandra and Bax 1997a; Tjandra et al. 1997; Luy and Marino 2001a). However, in the presence of differential relaxation it turns out that one of the two doublet lines can be broadened to an extent that makes these experiments rather unfavorable for the extraction of coupling constants. In this case, two classes of experiments referred to as *J*-modulated (Tjandra and Bax 1997b; Fehér et al. 2003) and

J. Furrer
Organisch-Chemisches Institut, Universität Heidelberg, Im
Neuenheimer Feld 270, 69120 Heidelberg, Germany

J. Furrer · M. John · H. Kessler · B. Luy (✉)
Department Chemie: Organische Chemie II, Technische
Universität München, Lichtenbergstr. 4, 85747 Garching,
Germany
e-mail: Burkhard.Luy@ch.tum.de

J-evolved (JE-) spectroscopy (Luy and Marino 2003) have been shown to overcome the problems due to differential relaxation by simultaneously retaining TROSY-enhanced linewidths.

Besides differential linebroadening, also other factors affect the ability to measure one-bond heteronuclear couplings, like, for example, the spectral resolution. Spin state selective approaches like S³E (Meissner et al. 1997a, b), or IPAP (Ottiger et al. 1998a) show reduced multiplets when applied to uniformly ¹⁵N-labeled proteins, but are not optimized with respect to linewidth and are usually limited to two chemical shift dimensions. The inherent dispersion of RDCs as an additional way to enhance the resolution is not exploited at all. Here we present 3D *J*-evolution-based experiments which retain chemical shift resolution in 2D planes and yield improved resolution in the additional (*J*+*D*)-dimension. The linewidths in this third dimension are studied by comparing several pulse sequences that also include the application of a BIRD^{*d,X*}-element.

As reported previously, *J*-modulated experiments can be improved using a BIRD^{*d,X*} element during the coupling evolution period (Uhrín et al. 1993; Fehér et al. 2003; Kövér and Batta 2004; Kövér and Forgó 2004). For amide groups, for example, the overall experiment duration is extended by $1/J_{\text{HN,N}}$, but refocusing of ¹H,¹H and long-range ¹H,¹⁵N couplings during the *J*-evolution period reduces the signal decay and/or undesired oscillations in the time domain. In the frequency domain this corresponds to a simplification of the multiplet pattern, leading in favorable cases to collapse to a single narrow line that compensates for losses during the BIRD^{*d,X*}-element. This improves the situation especially for partially aligned samples where the multitude of additional through-space homonuclear and heteronuclear couplings usually leads to strongly broadened multiplets. Several experiments are introduced and demonstrated on a cyclic pentapeptide, PA₄, and a small helical protein, Saposin C.

Theory

J-evolution based experiments

Five different experiments based on the JE-TROSY approach (Luy and Marino 2003) shall be introduced and compared. The experiments are designed for measuring one-bond ¹H,¹⁵N-couplings of amide groups with maximized resolution due to the sum of scalar

couplings and RDCs ($^1J_{\text{HN,N}} + D_{\text{HN,N}}$). The pulse sequences are shown in Fig. 1: the conventional JE-HSQC experiment with hard or selective ¹H-refocusing pulse during the *J*-evolution period (Fig. 1A), the counterpart JE-N-HSQC with the *J*-evolution on the ¹⁵N nuclei (Fig. 1B), and the corresponding JE-BIRD^{*d,X*}-HSQC (Fig. 1C) and JE-N-BIRD^{*d,X*}-HSQC (Fig. 1D) experiments with an additional BIRD^{*d,X*} element as described in Uhrín et al. (1993). The major differences between the five experiments shown in Fig. 1 are the couplings evolving and the type of nucleus subject to transverse relaxation during the *J*-evolution period *t*₁. The evolving couplings are summarized in Table 1: While basically all ¹H,¹H- and ¹H-¹⁵N-couplings contribute to the multiplet pattern in the simple JE-HSQC variant with the hard refocusing pulse, most of them are already removed by the application of a selective proton refocusing pulse in the center of *t*₁. However, best suppression of unwanted scalar couplings and RDCs during *t*₁ is achieved by applying a BIRD^{*d,X*} filter element (Table 1). Generally, ¹⁵N-evolved *t*₁-periods with relatively longer *T*₂ relaxation times of the nitrogen atoms lead to narrower lines in proteins and are therefore preferred.

Since evolution of chemical shifts does not occur during the *t*₁ period, conventional quadrature detection schemes such as the States or TPPI methods are not required. A complex Fourier transform along the *J*-dimension using conventional NMR processing software can still be performed if the acquired real part of the spectrum is extended by an imaginary part consisting of zeros as described in (Luy and Marino 2003). The resulting pure phase ¹*J*_{HN,N}-doublets are either in- or antiphase, depending on whether the *J*-evolution period starts with maximum (as in the JE-N-HSQC and JE-N-BIRD^{*d,X*}-HSQC) or minimum (i.e., zero as in the JE-HSQC and the JE-BIRD^{*d,X*}-HSQC variants) initial magnetization. In the presented pulse schemes and in particular the scheme using a selective ¹H-refocusing pulse, the first data point in the *J*-dimension (*t*₁ = 0) is not directly accessible and can be omitted, if a 360° first order phase correction is applied to the *J*-spectrum.

The BIRD^{*d,X*}-element

In the following, the BIRD^{*d,X*}-element with its ability to significantly simplify multiplet patterns shall be analyzed more closely using the appropriate nomenclature for the participating nuclei (Uhrín et al. 1993): a BIRD filter 90°(¹H)-δ-180°(¹H,X)-δ-90°(¹H)

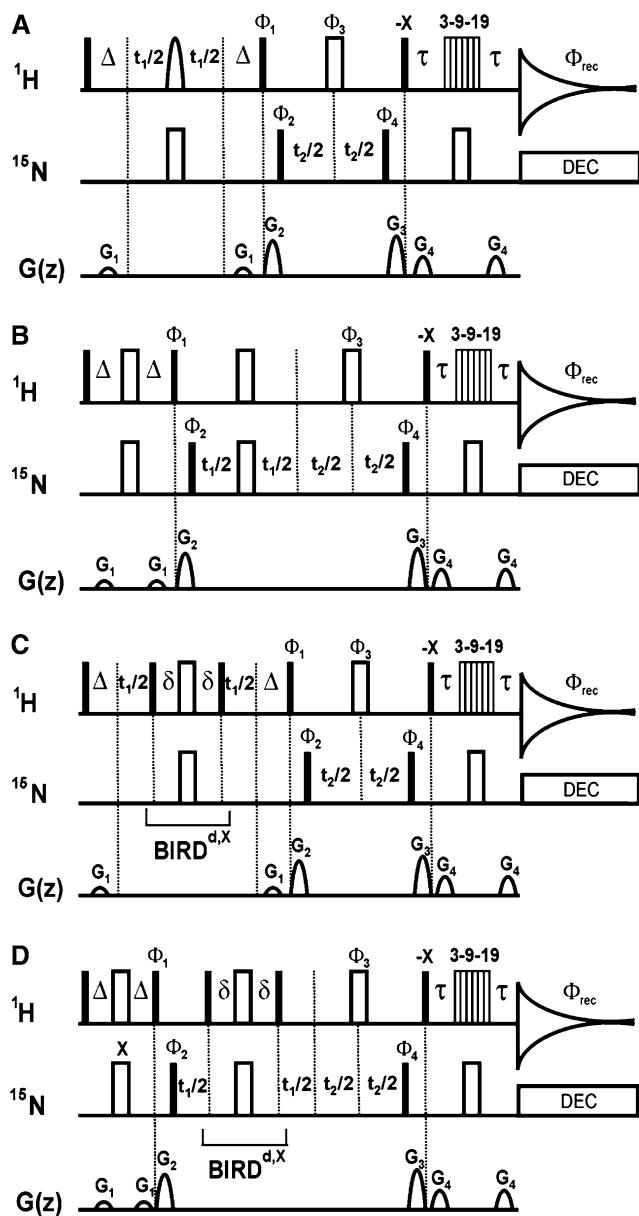


Fig. 1 Pulse schemes for 3D JE-HSQC (A), 3D JE-N-HSQC (B), 3D JE-BIRD^{d,X}-HSQC (C), and 3D JE-N-BIRD^{d,X}-HSQC (D) experiments. All experiments are based on the FAST-HSQC detection scheme (Mori et al. 1995). Narrow filled pulses correspond to flip angles of 90° and wide open to 180°. Composite pulse (GARP Shaka et al. 1985) ¹⁵N decoupling was used during acquisition. The first 180° ¹H pulse in the center of the *t*₁ evolution period in the 3D JE-HSQC (A) (drawn as a Gaussian shape) can be applied either as hard or selective pulse, to decouple or not decouple ¹H–¹H couplings between amide and aliphatic protons. The composite WATERGATE pulse is a 3-9-19 scheme (Piotto et al. 1992; Sklenar et al. 1993) with pulse intervals of 100 μs. Delay durations: Δ = 2.75 ms; δ = 5.5 ms; τ = 1.3 ms for a total preparation and refocusing time of 5.5 ms. For all experiments, the increment in the *J*-dimension is adjusted to 5.5 ms. The first delay in the *J*-dimension is adjusted to 5.5 ms for experiments (A) and (C) (corresponding to the time increment used in the *J*-evolution period) and 3 μs for experiments (B) and (D). Phase sensitive spectra in the *J*-dimension were achieved using the procedure described in (Luy and Marino 2003). States quadrature detection is used in the *J* dimension. Phases are: φ1 = *y*; φ2 = *x*, -*x*; φ3 = *x*, *x*, -*x*, -*x*; φ4 = *x*, *x*, *x*, *x*, -*x*, -*x*, -*x*, -*x*; Receiver = *x*, -*x*, *x*, -*x*, -*x*, *x*, -*x*, *x*. Sine-bell shaped pulse field gradients (1 ms each, *z*-axis) have strengths (in % of max. strength): G1:10; G2: -10; G3: 80; G4: 8.1

generally works as a selective 180° pulse which is able to distinguish the heteronucleus *X*, its directly bound protons *d*, and all remotely bound protons *r*. Depending on the phases used for the 90° proton pulses, either combination of spins can selectively be inverted (Uhrín et al. 1993). For example, the BIRD^{d,X}-filter with all pulses applied with phase *x* selectively inverts the heteronucleus and the directly bound protons while leaving remote protons untouched. A product operator analysis of an *XI^dI^r* three spin system with the corresponding *J_{d,X}*, *J_{d,r}*, and *J_{r,X}* couplings, results for example in the transfer

$$\begin{aligned}
 I_x^d \xrightarrow{90_x^\circ(I)} & I_x^d \xrightarrow{\delta} I_x^d \cos \pi \delta^1 J_{d,X} \cos \pi \delta^n J_{d,r} + 2I_y^d X_z \sin \pi \delta^1 J_{d,X} \cos \pi \delta^n J_{d,r} \\
 & + 2I_y^d I_z^d \cos \pi \delta^1 J_{d,X} \sin \pi \delta^n J_{d,r} - 4I_x^d I_z^d X_z \sin \pi \delta^1 J_{d,X} \sin \pi \delta^n J_{d,r} \\
 180_x^\circ(I,X) \xrightarrow{\delta} & I_x^d \cos \pi \delta^1 J_{d,X} \cos \pi \delta^n J_{d,r} + 2I_y^d X_z \sin \pi \delta^1 J_{d,X} \cos \pi \delta^n J_{d,r} \\
 & + 2I_y^d I_z^d \cos \pi \delta^1 J_{d,X} \sin \pi \delta^n J_{d,r} - 4I_x^d I_z^d X_z \sin \pi \delta^1 J_{d,X} \sin \pi \delta^n J_{d,r} \\
 \xrightarrow{\delta} & I_x^d \cos 2\pi \delta^1 J_{d,X} \cos 2\pi \delta^n J_{d,r} + 2I_y^d X_z \sin 2\pi \delta^1 J_{d,X} \cos 2\pi \delta^n J_{d,r} \\
 & + 2I_y^d I_z^d \cos 2\pi \delta^1 J_{d,X} \sin 2\pi \delta^n J_{d,r} - 4I_x^d I_z^d X_z \sin 2\pi \delta^1 J_{d,X} \sin 2\pi \delta^n J_{d,r} \\
 90_x^\circ(I) \xrightarrow{\delta} & I_x^d \cos 2\pi \delta^1 J_{d,X} \cos 2\pi \delta^n J_{d,r} + 2I_z^d X_z \sin 2\pi \delta^1 J_{d,X} \cos 2\pi \delta^n J_{d,r} \\
 & - 2I_x^d I_y^d \cos 2\pi \delta^1 J_{d,X} \sin 2\pi \delta^n J_{d,r} + 4I_x^d I_y^d X_z \sin 2\pi \delta^1 J_{d,X} \sin 2\pi \delta^n J_{d,r}
 \end{aligned}$$

Table 1 Couplings contributing to the multiplet pattern during the J -evolution period of the corresponding experiments of Fig. 1

	JE-HSQC (hard)	JE-HSQC (selective)	JE-N-HSQC	JE-BIRD ^{d,X} -HSQC	JE-N-BIRD ^{d,X} -HSQC
Transverse nucleus	¹ HN	¹ HN	¹⁵ N	¹ HN	¹⁵ N
¹ J _{HN,N}	Yes	Yes	Yes	Yes	Yes
ⁿ J _{HN,HN} / ^m J _{N,N} ^a	Yes	Yes	Only U- ¹⁵ N ^b	Only U- ¹⁵ N ^b	Only U- ¹⁵ N ^b
ⁿ J _{HN,N}	Only U- ¹⁵ N ^b	Only U- ¹⁵ N ^b	Yes	Only U- ¹⁵ N ^b	Only U- ¹⁵ N ^b
ⁿ J _{HN,Haliph} / ^m J _{N,Haliph} ^a	Yes	No	Yes	No	No
ⁿ J _{HN,Harom} / ^m J _{N,Harom} ^a	Yes	Yes	Yes	No	No

^a depending on the respective transverse nucleus

^b the corresponding couplings are only active in uniformly ¹⁵N-labeled molecules

¹ J_{HN,N}: the direct one-bond heteronuclear (¹J_{HN,N} + D_{HN,N})-coupling of interest

ⁿ J_{HN,HN}: short and long-range homonuclear scalar and/or dipolar couplings between ¹⁵N-attached protons

ⁿ J_{N,N}: long-range ¹⁵N,¹⁵N scalar couplings or RDCs

ⁿ J_{HN,N}: long-range heteronuclear scalar and/or dipolar couplings to the ¹⁵N-attached proton or ¹⁵N of interest

ⁿ J_{HN,Haliph}, ⁿJ_{N,Haliph}: homonuclear ¹H,¹H and long-range heteronuclear scalar and/or dipolar couplings from aliphatic protons to the amide group of interest

ⁿ J_{HN,Harom}, ⁿJ_{N,Harom}: homonuclear ¹H,¹H and long-range heteronuclear scalar and/or dipolar couplings from aromatic protons covered by the selective refocusing pulse during t_1 to the amide group of interest

For the ideal delay $2\delta = 1/(^1J_{d,X})$ and negligible homonuclear and heteronuclear long-range couplings, transfers for the derived and further transverse components simplify to

$$\begin{array}{llll}
 I_x^d & \longrightarrow & -I_x^d & I_y^d \longrightarrow I_y^d \\
 2I_x^d X_z & \longrightarrow & 2I_x^d X_z & 2I_y^d X_z \longrightarrow -2I_y^d X_z \\
 I_x^r & \longrightarrow & I_x^r & I_y^r \longrightarrow I_y^r \\
 2I_x^r X_z & \longrightarrow & 2I_x^r X_z & 2I_y^r X_z \longrightarrow 2I_y^r X_z \\
 X_x & \longrightarrow & -X_x & X_y \longrightarrow X_y \\
 2I_z^d X_x & \longrightarrow & 2I_z^d X_x & 2I_z^d X_y \longrightarrow -2I_z^d X_y
 \end{array}$$

In this case, original I^d and X single quantum coherences are inverted as if a 180_y° pulse would have been applied on both spins, while the remote proton I^r is left unchanged.

However, if the matching condition is not fulfilled or if considerably strong homonuclear or heteronuclear long-range couplings are present, initial single quantum coherences get partially converted into ZQ/DQ coherences or other terms that evolve with different frequencies than the original single quantum coherence. In the appendix, a detailed derivation of transfer properties of important coherences in J -evolution periods is given. The main effect of mismatched delays is a decrease of signal intensities for the original single quantum terms.

The strongest reduction in signal intensity for partially aligned samples is introduced by the dispersion due to RDCs, where the dipolar coupling contribution inevitably results in mismatched delays. Based on the product operator analysis, we can assume an average reduction due to delay mismatch of $0.5^*(1 - \cos(2\pi\delta^1J_{d,X}))$ (see appendix and Pham et al. 2002),

which translates into $0.5^*(1 - \cos(2\pi\delta(^1J_{NH,N} + D_{NH,N})))$ for partially aligned amide groups. A 10% (20%) mismatch of the coupling compared to the actual coupling $2\delta = 1/(^1J_{d,X})$ used in the experiment, for example, leads to a signal loss of 3% (10%).

Additional reduction of signal intensities by the product $0.5^*\Pi(1 - \cos(2\pi\delta^nJ_{d,r}))$ over all remotely coupled protons results from homonuclear coupling evolution (see appendix). Heteronuclear long-range couplings do not affect transverse proton operators during the BIRD^{d,X} element, but reduce signal intensities by the product $\Pi(1 - \cos(2\pi\delta^nJ_{r,X}))$ over all long-range couplings if operators of the heteronucleus are transverse during J -evolution periods (see appendix). However, homonuclear and long-range heteronuclear couplings are typically small compared to the heteronuclear one-bond coupling and the scaling should be negligible. In addition, the loss of magnetization can be overcompensated by the effective decoupling with respect to the remote spins, leading to even increased net peak heights due to reduced multiplet-widths.

It should be noted, that only remote protons are decoupled. If more than one proton is directly attached to the heteronucleus, as for example in CH₂, CH₃, or NH₂ groups, all protons are inverted equally and homonuclear couplings between the direct protons will still evolve during J -evolution periods and contribute to the multiplet pattern (see also Pham et al. 2002). Equally, homonuclear and long-range heteronuclear couplings between two spin groups with the same type of heteronucleus, as for example an amide group coupled to another amide group, will not be refocused by the BIRD^{d,X} element. Instead, heteronuclear

couplings to further nuclei during t_1 , as for example ^{13}C in ^{15}N , ^{13}C -labeled compounds, are decoupled by an ^1H , ^{15}N -BIRD d,X -element and do not contribute to the signal multiplicity.

Due to the central hard 180° pulses on both the protons and the heteronucleus, α and β states are interconverted, and differential line broadening due to DD-CSA or DD-DD cross-correlated relaxation is suppressed by the BIRD-filter. Homonuclear ^1H , ^1H DD-CSA cross-correlation effects in the experiments using ^1H coherence during t_1 are expected to be weak and therefore negligible.

Materials and methods

Sample preparation

Cyclo(-D-Pro-Ala-Ala-Ala-Ala-) (referred to as PA₄) was chemically synthesized using uniformly ^{15}N , ^{13}C -labeled Fmoc-Ala and standard methods for cyclization (Kessler 1982; Mierke et al. 1994). The sample used for measurements was prepared in DMSO- d_6 with a final concentration of 2 mM. Uniformly ^{15}N -labeled human Saposin C with hexa-histidine tag at the C-terminus was expressed in the methylotrophic yeast *Pichia pastoris* according to a procedure analogous to that described elsewhere (Wendeler et al. 2004). The protein was concentrated to a 1.4 mM solution and buffer conditions were adjusted to 90% H₂O/10% D₂O with 50 mM phosphate buffer, pH 7.0. In a further step, the sample was mixed with filamentous Pf1-phage to a final concentration of 13 mg/ml for partial alignment.

NMR spectroscopy

All spectra of PA₄ were recorded at 300 K on a Bruker DMX750 spectrometer as 2D experiments (omitting the ^{15}N dimension) with a data matrix of 256×2048 points and acquisition times of 1406 ms (t_1 , J) and 102 ms (t_3 , ^1H) with 2 scans per FID. An artificial imaginary part in the indirect dimension consisting of zeros was added to each spectrum to a final size of 512×2048 points before complex Fourier transformation (for detailed description of the processing procedure see Luy and Marino 2003).

All experiments on Saposin C were acquired at 310 K. JE-Spectra of the aligned sample were recorded as a $48 \times 64 \times 2048$ data matrix with maximum acquisition times of 240 ms (t_1 , J -dimension), 24 ms (t_2 , ^{15}N), and 103 ms (t_3 , ^1H) using 32 scans per

FID for an overall measurement time of 35 h per experiment. Addition of a zero imaginary part in the J -dimension and zero-filling to $128 \times 96 \times 2048$ points was applied prior to Fourier transform. Processing and analysis were carried out using the software NMRpipe (Delaglio et al. 1995) and Sparky (Goddard and Kneller, University of California; Kneller and Kuntz 1993). For comparison, IPAP-HSQC spectra (Ottiger et al. 1998a) were recorded on both unaligned and aligned protein sample to yield $^1J_{\text{HN,N}}$ and $^1J_{\text{HN,N}} + D_{\text{HN,N}}$ couplings, respectively. Each spectrum had a time domain size of 512×1024 , corresponding to acquisition periods of 190 ms (^{15}N) and 51 ms (^1H), which was zero-filled to a size of 1024×1024 prior to Fourier transform. 128 scans per increment were added for a total experiment duration of 36 h each.

Results

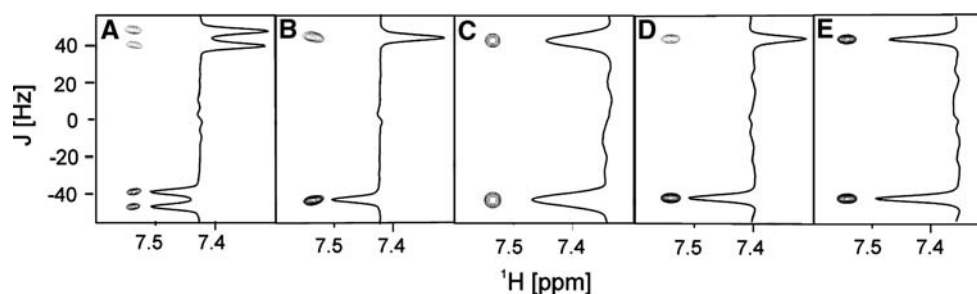
PA₄

The five experiments of Fig. 1 were recorded on the ^{15}N , ^{13}C -labeled cyclic pentapeptide PA₄ to study the signal width in the J -spectra due to ^1H - ^1H and long-range ^1H - ^{15}N couplings. The results are illustrated in Fig. 2: The $^1J_{\text{HN,N}}$ antiphase doublet pattern in the non-selective JE-HSQC is further split by a large $^3J_{\text{HN,H}\beta}$ coupling of approximately 9 Hz (Fig. 2A). Similarly, the signal width observed in the JE-N-HSQC experiment is clearly increased compared to the JE-N-BIRD d,X -HSQC due to long-range $^2J_{\text{N,H}\alpha}$, $^3J_{\text{N,H}\beta}$, and interresidual $^3J_{\text{N,H}\alpha}$ couplings (Fig. 2C). The selective JE-HSQC and the BIRD d,X -experiments all show comparable linewidths of approximately 4 Hz (Fig. 2B, D, E).

Saposin C

Three of the five experiments, namely the JE-BIRD d,X -HSQC, JE-N-HSQC, and JE-N-BIRD d,X -HSQC sequences were applied to the ^{15}N -labeled protein Saposin C aligned in Pf1-phage. In partially oriented biomolecules, further line broadening is expected not only due to faster transverse relaxation, but also due to the occurrence of residual long range dipolar interactions in addition to the scalar couplings mentioned above. Traces of the resulting J -dimensions in the acquired spectra are shown in Fig. 3 for a typical residue. Now the signal width obtained for J -evolution with ^{15}N being in the

Fig. 2 Contour plots of and slices through the cross peak of Ala₅ in the JE-HSQC with hard (A) and selective (B) inversion pulse, JE-N-HSQC (C), JE-BIRD^{d,X}-HSQC (D), and JE-N-BIRD^{d,X}-HSQC (E) acquired on the cyclic pentapeptide PA₄



transverse plane (Fig. 3B) is significantly smaller than for the experiment with transverse ¹H magnetization (Fig. 3A), and the BIRD^{d,X} filter provides an additional reduction to approximately 5 Hz (Fig. 3C). For comparison, ¹⁵N-linewidths of typically 7 Hz for the downfield and 10 Hz for the upfield doublet components were observed in IPAP-HSQC spectra of the same sample.

Residual dipolar couplings measured from both the JE-N-BIRD^{d,X}-HSQC and the IPAP method were basically identical, resulting in the typical zig-zag wave pattern of five α -helices. A special case of determination of coupling constants is shown in Fig. 4. While signals for L70, D30, Y4 (tentative assignment), and F32 are partially overlapped in the IPAP-HSQC spectra so that coupling constants can only be measured with enlarged error, the signals of all four residues are resolved in the JE-N-BIRD^{d,X}-HSQC due to the additional dispersion in the *J*-dimension. 71 ¹H,¹⁵N-RDCs of Saposin C have been measured with the JE-N-BIRD^{d,X}-HSQC. In Fig. 5, the experimental couplings are plotted against RDCs fitted to the structural model with pdb-entry 1M12 (De Alba et al. 2003) using the program PALES. The graph shows excellent agreement of measured versus backcalculated RDCs with a correlation factor $R^2 = 0.976$.

Resolution enhancement in Saposin C due to $D_{\text{HN,N}}$ dispersion

All $^1J_{\text{HN,N}}$ -coupling constants are in the range of 91–96 Hz, with an average value close to 93 Hz. Therefore the effective $^1J_{\text{HN,N}} + D_{\text{HN,N}}$ couplings in the aligned sample roughly translate into the $D_{\text{HN,N}}$ couplings of the corresponding amide groups. Figure 6 shows three slices from the JE-N-BIRD^{d,X}-HSQC spectrum at (*J*+*D*)-values of 72, 92, and 109 Hz, corresponding to RDCs of approximately –21, –1, and +16 Hz. Compared to the ¹H,¹⁵N-HSQC of the unaligned protein (Fig. 6A), the slices show a significantly reduced number of cross peaks with almost all overlaps nicely separated in the *J*-dimension. Only residues V3 ($D_{\text{HN,N}} = 5$ Hz), A31 ($D_{\text{HN,N}} = 9$ Hz), and V51 ($D_{\text{HN,N}} = -7$ Hz) are present in two 2D slices, because they have intermediate RDCs right between the selected frequencies. These residues are also special in the way that their signals are relatively strong, which lets them be present in a relatively wide range of *J*-slices despite their narrow lines.

Since the axes of Saposin C's α -helices point in different directions in 3D space, each helix has a characteristic range of RDCs that can be partially separated in the *J*-dimension. This way N-H-vectors of helices α_1 and α_2 are found in both 2D slices

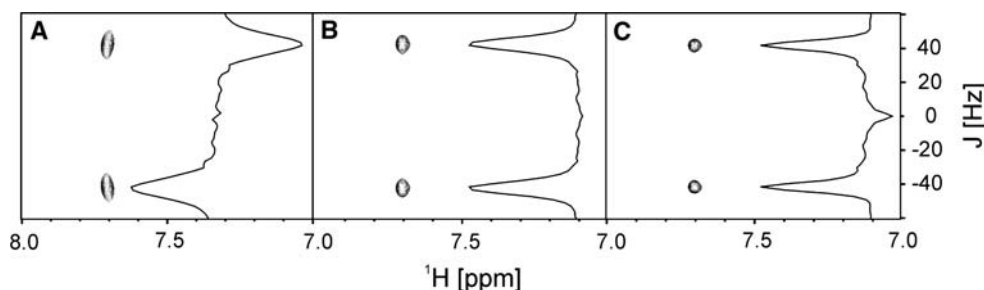


Fig. 3 Contour plots of and slices through residue H76 extracted from JE-BIRD^{d,X}-HSQC (A), JE-N-HSQC (B) and JE-N-BIRD^{d,X}-HSQC (C) experiments applied to Saposin C, a

medium sized protein. The isolated residue H76 as a typical cross peak is shown to compare the relative signal widths in the JE-dimension

Fig. 4 The most crowded region of the ^1H , ^{15}N -HSQC spectrum of the unaligned sample of Saposin C is shown in (A) (see also Fig. 6A). In the corresponding regions of the two IPAP-HSQC subspectra (overlayed using solid and dashed lines) RDCs cannot be measured due to partial overlap of four residues (B). In the 2D J - ^1H -planes of the 3D JE-N-BIRD d,X -HSQC at nitrogen chemical shifts of 118.0 and 119.0 ppm, however, the signals are separated and couplings can be derived (C,D). The assignment of Y4 is only tentative and therefore indicated with a question mark

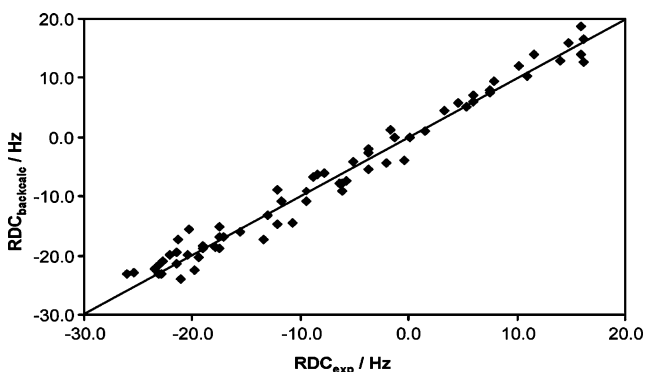
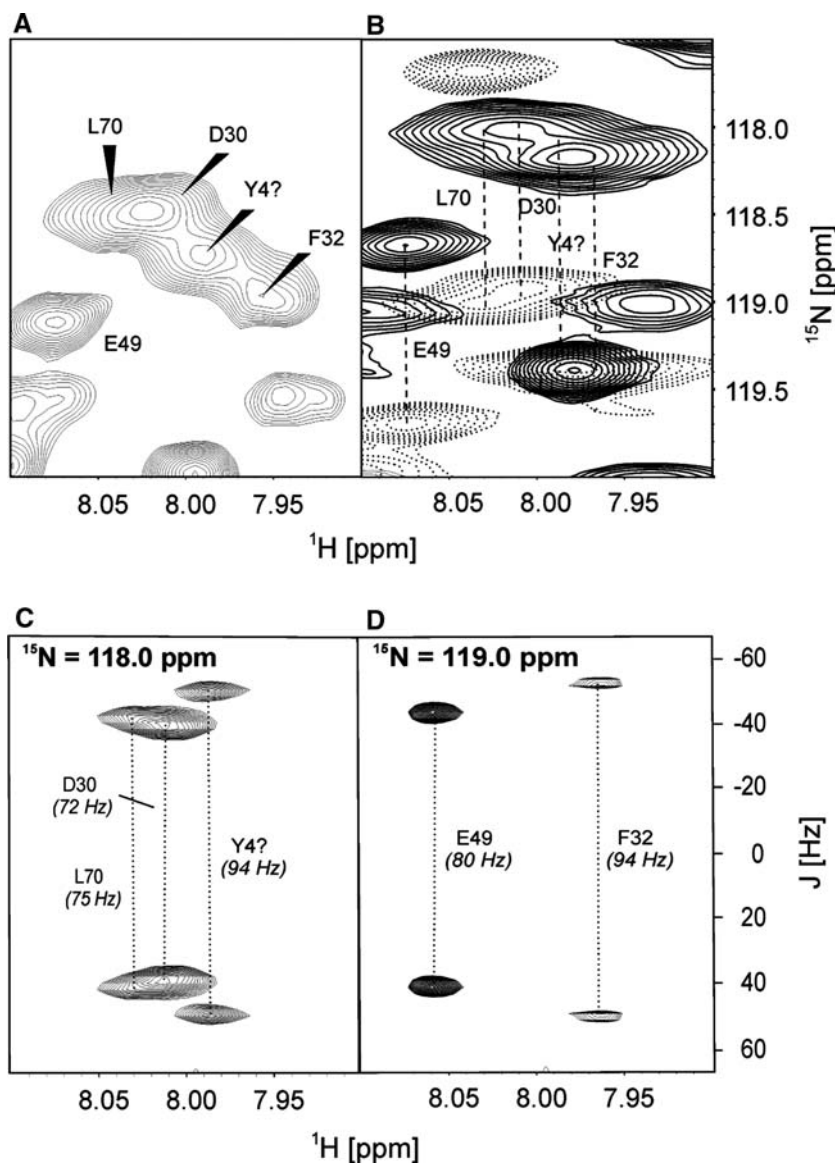


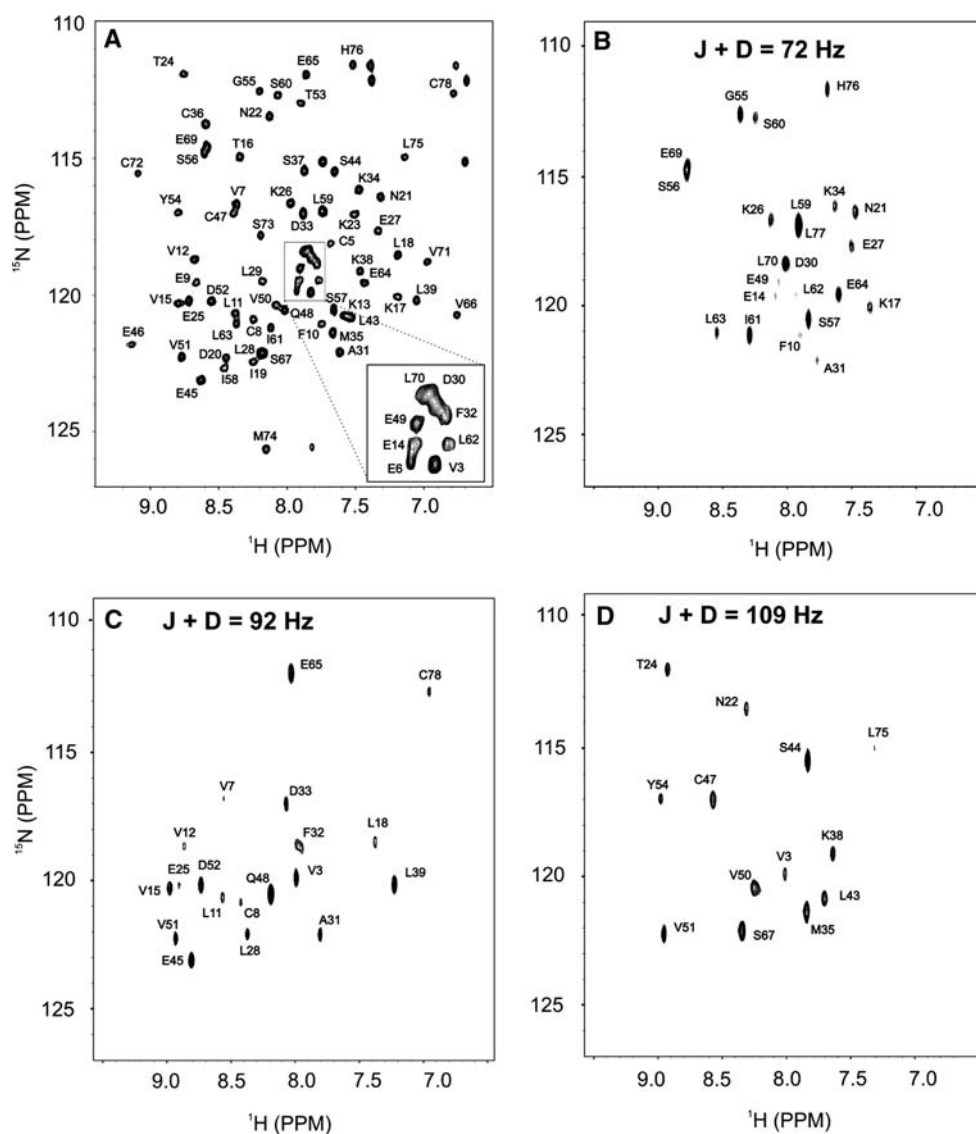
Fig. 5 Correlation plot of experimental RDCs obtained from the JE-N-BIRD d,X -HSQC versus the corresponding back-calculated RDCs using the structure published in (De Alba et al. 2003)

corresponding to effective ($J+D$) couplings of 72 and 92 Hz, while helix $\alpha 3$ can be found at 92 and 109 Hz, and helix $\alpha 5$ at 72 and 109 Hz (Fig. 7). Helix $\alpha 4$ is only present in the 2D-plane at ($J+D$) = 72 Hz.

Discussion

The results presented demonstrate that J -evolution combined with the BIRD d,X element (Uhrin et al. 1993) provides a method for accurate measurement of heteronuclear one-bond couplings in biomacromolecules with enhanced resolution due to $D_{\text{HN,N}}$ RDCs. Compared to conventional methods for coupling determination like the IPAP-HSQC, the

Fig. 6 ^1H , ^{15}N -HSQC of unaligned Saposin C (A) and several ^1H , ^{15}N -planes at different ($J+D$) frequencies from the 3D JE-N-BIRD d,X -HSQC spectrum acquired on Saposin C partially aligned in Pf1 phage (B–D). The aligned Saposin C generally shows slightly broader cross peaks in the ^{15}N -dimension because of the lower number of increments acquired, but due to RDC-induced dispersion in the ($J+D$)-dimension overall resolution is significantly improved

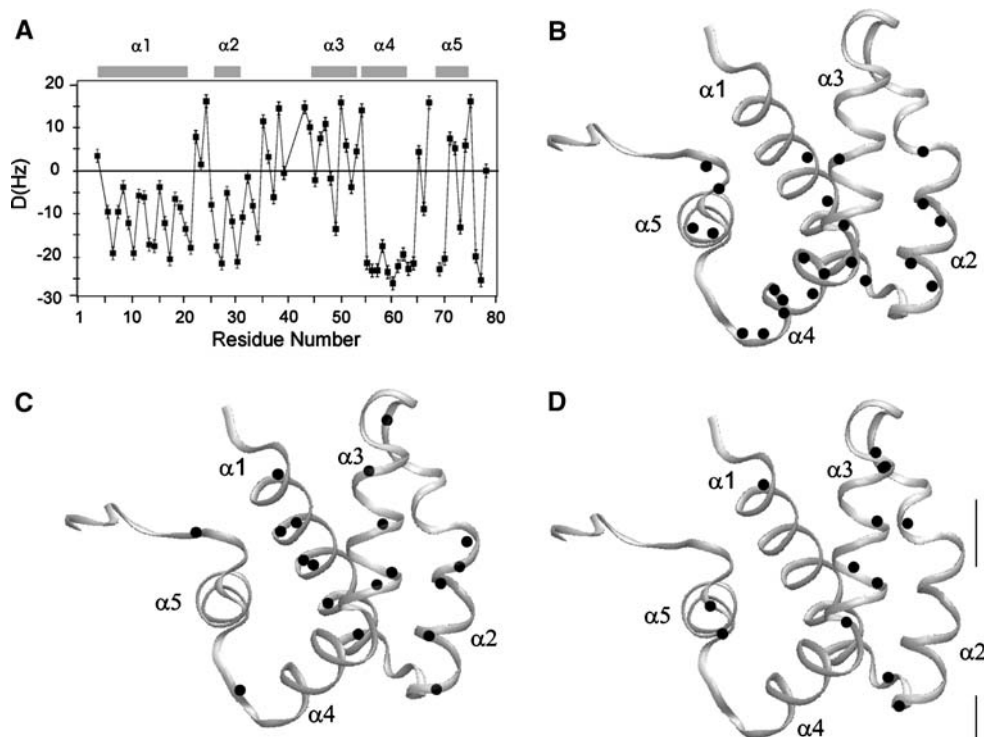


proposed 3D JE-N-BIRD d,X -HSQC has the disadvantage of an additional dimension and therefore an increased minimum measurement time. As long as all desired signals are resolved in the 2D spectra, the additional measurement time needed for the J -evolved spectrum should not be wasted. In principle, resolution in the indirect dimension of IPAP-HSQC experiments could also significantly be improved by a BIRD r -filter which would refocus all long-range ($^nJ_{\text{HN,N}} + D_{\text{HN,N}}$) couplings during t_1 and therefore decrease the linewidth (as e.g. used in Fehér et al. 2003). In this case the resulting spectrum is still a 2D spectrum. The full resolution enhancement with respect to chemical shift and RDC dispersion, however, is only met in a separate dimension as presented here. It should be noted that 7 one-bond couplings in Saposin C could be measured in the JE-N-BIRD d,X -

HSQC experiment that could not be resolved in the corresponding IPAP-HSQC (Fig. 4 and John et al. 2006). This represents approximately 10% of the amide one-bond couplings.

In J -evolution periods with the BIRD d,X element most indirect couplings as well as B_0 -inhomogeneities are refocused. Additional spectral resolution in the J -dimension can therefore be achieved in all cases where the ($J+D$)-dispersion is larger than the “relaxation only”-linewidth. As shown in Fig. 4, this allows the measurement of coupling constants for residues with resonances partially overlapping in the ^1H as well as the ^{15}N dimensions. This property of the proposed experiments is especially important, since dipolar coupling constants can be varied relatively easily by adjusting the degree of alignment or the kind of alignment medium used. For the majority of residues

Fig. 7 RDCs of Saposin C and the occurrence of structural elements in the different JE(N)-BIRD^{d,x}-HSQC planes. The sequence plot shows the typical zig-zag lines for the α -helices in Saposin C (A). For each of the three extracted ¹H,¹⁵N-planes of Fig. 6B–D the corresponding cross peaks are indicated as black points in the structure of Saposin C at the position of the amide nitrogen (B–D)



with two N–H internuclear vectors pointing in different directions it should therefore be possible to resolve even complete ¹H and ¹⁵N chemical shift degeneracy via the ($J+D$)-dimension.

The limits of the JE-approach with respect to molecular size have already been discussed previously (Luy and Marino 2003). For very large molecules (larger than approximately 30 kDa) with short T_2 relaxation times the application of the BIRD^{d,x}-element might not be feasible because of the loss of signal during the additional delays. This loss is expected to be significantly larger for the experiments, in which the magnetization during the J -evolution resides on ¹H ($T_2 \approx 20$ ms for Saposin C) rather than ¹⁵N ($T_2 \approx 140$ ms for Saposin C). At high molecular weight, however, the natural linewidth will by far exceed the signal width contribution of small heteronuclear or ¹H-¹H homonuclear couplings, such that only a minor resolution enhancement is expected from the inclusion of the BIRD^{d,x}-element. In this case, the corresponding TROSY-type pulse sequences (Luy and Marino 2003) with selective ¹H refocusing pulses applied during t_1 seems to be the more appropriate choice.

The number of time increments in the J -evolved dimension of a JE-N-BIRD^{d,x}-HSQC should be chosen carefully. Additional resolution is always traded in for lower sensitivity, and the maximum t_1 time should be adjusted to the expected linewidth in the ($J+D$)-dimension. For a full-width-at-half-height linewidth of 5 Hz, 240 ms for the maximum t_1 is a reasonable

choice. For molecules with longer correlation times and increased linewidth, the number of t_1 -increments should be reduced accordingly.

It should be noted that an ideal performance of the BIRD^{d,x} element is expected only for a small window of ($J+D$)-couplings close to the inverse of the chosen delay. Nevertheless, for none of the couplings in the entire range of 68–110 Hz present in aligned Saposin C phase-twisting or other artifacts were encountered, and the expected reduction in intensity is in all cases less than 15%. For stronger alignments and therefore a wider range of ($J+D$)-couplings such problems might well arise. To prevent evolution of homonuclear proton antiphase magnetization during the BIRD^{d,x} element, it might be replaced by a CAGEBIRD^{d,x} element (koskela et al. 2004) which uses the homonuclear Hartmann Hahn conditions created by CPMG transfer elements for retaining inphase magnetization (Luy and Marino 2001b)

In favorable cases the dispersion due to RDCs in aligned samples might be a useful tool to distinguish specific parts of a molecule or aid in the ¹⁵N-HSQC assignment, as RDCs have been used previously for the resonance assignment of proteins with (Jung and Zweckstetter 2004a, 2004b) and without (Jung et al. 2004) known structure. An example is shown in Fig. 7, where RDC-based dispersion can be used to separate cross peaks originating from different α -helices.

The JE-approach, of course, is not limited to ¹⁵N-labeled proteins and peptides, but should be easily

transferable to other labeling-schemes or even unlabeled samples. For other classes of biomolecules like nucleic acids and carbohydrates, overlap is a very serious problem and JE-resolved spectra exploiting the possibilities of RDC-dispersion could play an important role in obtaining unambiguous assignments. It might also be very useful in the context of small organic molecules, where new alignment media and analytical methods currently open a variety of possible applications (Yan et al. 2003, 2004; Thiele 2004, 2005; Haberz et al. 2005; Klages et al. 2005; Kobzar et al. 2005; Luy et al. 2005).

For isotropic samples with no additional resolution due to RDCs, the proposed experiments can only provide very limited additional resolution. Amide $^1J_{\text{HN,N}}$ coupling constants are known to have little variation, as well as most aliphatic $^1J_{\text{HC}}$ coupling constants. The situation is different for aromatic systems with a wide range of $^1J_{\text{HC}}$ coupling constants, where a corresponding JE-C-BIRD d,X -HSQC experiment could already provide additional resolution when applied to an unaligned sample.

The ($J+D$)-dimension can be principally incorporated in high dimensionality approaches like FDM (Mandelstam et al. 1998), GFT (Kim and Szyperski 2003), projection reconstruction (Kupce and Freeman 2003), or covariance NMR (Bruschweiler and Zhang 2004) to further reduce experiment times.

Conclusion

In summary, the usefulness of J -evolution spectroscopy for the determination of large one-bond heteronuclear

coupling constants, as previously introduced in the JE-TROSY approach, could be demonstrated also for small to medium-sized biomolecules. With a BIRD d,X -element during J -evolution the linewidth for the protein Saposin C could be reduced significantly in the J -dimension which not only allowed the accurate measurement of $^1J_{\text{HN,N}} + D_{\text{HN,N}}$ couplings, but also resulted in a novel way to increase signal dispersion in partially aligned samples. The limiting resolution is no longer determined by chemical shifts alone but additionally by the dispersion of RDCs which can be scaled over a wide range by the choice of alignment medium and alignment strength.

Acknowledgment B.L. and H.K. thank the Fonds der Chemischen Industrie and the Deutsche Forschungsgemeinschaft (Emmy Noether fellowship LU 835/1-1; Ke 147/37-1) for financial support. We thank Martin Sukopp (Stanford University, USA) for the synthesis of PA $_4$, Michaela Wendeler (National Cancer Institute, Frederick MD, USA) and Konrad Sandhoff (Universität Bonn, Germany) for kindly providing Saposin C and Jochen Klages (TU München, Germany) for help with the assignment of Saposin C.

Appendix

Neglecting strong coupling artifacts, the evolution of transverse operators during a BIRD d,X element applied to a three spin system consisting of one heteronucleus X , one directly coupled proton spin I^d , and one remotely coupled proton spin I^r with the corresponding couplings $J_{d,X} > J_{d,r} \approx J_{r,X}$, results in the following transfers:

$$\begin{aligned}
 I_x^d &\longrightarrow I_x^d \cos 2\pi\delta^1 J_{d,X} \cos 2\pi\delta^n J_{d,r} + 2I_z^d X_z \sin 2\pi\delta^1 J_{d,X} \cos 2\pi\delta^n J_{d,r} \\
 &\quad - 2I_z^d I_y^r \cos 2\pi\delta^1 J_{d,X} \sin 2\pi\delta^n J_{d,r} + 4I_x^d I_y^r X_z \sin 2\pi\delta^1 J_{d,X} \sin 2\pi\delta^n J_{d,r} \\
 I_y^d &\longrightarrow I_y^d \\
 2I_x^d X_z &\longrightarrow -2I_x^d X_z \cos 2\pi\delta^1 J_{d,X} \cos 2\pi\delta^n J_{d,r} - I_z^d \sin 2\pi\delta^1 J_{d,X} \cos 2\pi\delta^n J_{d,r} \\
 &\quad + 4I_z^d I_y^r X_z \cos 2\pi\delta^1 J_{d,X} \sin 2\pi\delta^n J_{d,r} - 2I_x^d I_y^r \sin 2\pi\delta^1 J_{d,X} \sin 2\pi\delta^n J_{d,r} \\
 2I_y^d X_z &\longrightarrow -2I_y^d X_z \\
 X_x &\longrightarrow X_x \cos 2\pi\delta^1 J_{d,X} \cos 2\pi\delta^1 J_{r,X} - 2I_y^d X_y \sin 2\pi\delta^1 J_{d,X} \cos 2\pi\delta^1 J_{r,X} \\
 &\quad - 2I_y^r X_y \cos 2\pi\delta^1 J_{d,X} \sin 2\pi\delta^1 J_{r,X} - 4I_y^d I_y^r X_x \sin 2\pi\delta^1 J_{d,X} \sin 2\pi\delta^1 J_{r,X} \\
 X_y &\longrightarrow -X_y \cos 2\pi\delta^1 J_{d,X} \cos 2\pi\delta^1 J_{r,X} - 2I_y^d X_x \sin 2\pi\delta^1 J_{d,X} \cos 2\pi\delta^1 J_{r,X} \\
 &\quad - 2I_y^r X_x \cos 2\pi\delta^1 J_{d,X} \sin 2\pi\delta^1 J_{r,X} + 4I_y^d I_y^r X_y \sin 2\pi\delta^1 J_{d,X} \sin 2\pi\delta^1 J_{r,X} \\
 2I_z^d X_x &\longrightarrow 2I_z^d X_x \cos 2\pi\delta^1 J_{r,X} \cos 2\pi\delta^n J_{d,r} - 4I_z^d I_y^r X_y \sin 2\pi\delta^1 J_{r,X} \cos 2\pi\delta^n J_{d,r} \\
 &\quad + 4I_x^d I_y^r X_x \cos 2\pi\delta^1 J_{r,X} \sin 2\pi\delta^n J_{d,r} - 2I_x^d X_y \sin 2\pi\delta^1 J_{r,X} \sin 2\pi\delta^n J_{d,r} \\
 2I_z^d X_y &\longrightarrow -2I_z^d X_y \cos 2\pi\delta^1 J_{r,X} \cos 2\pi\delta^n J_{d,r} - 4I_z^d I_y^r X_x \sin 2\pi\delta^1 J_{r,X} \cos 2\pi\delta^n J_{d,r} \\
 &\quad - 4I_x^d I_y^r X_y \cos 2\pi\delta^1 J_{r,X} \sin 2\pi\delta^n J_{d,r} - 2I_x^d X_x \sin 2\pi\delta^1 J_{r,X} \sin 2\pi\delta^n J_{d,r}
 \end{aligned}$$

If we assume that long-range heteronuclear and homonuclear couplings can be neglected during the BIRD^{d,X} element, the transfers can be simplified to

$$\begin{aligned} I_x^d &\longrightarrow I_x^d \cos 2\pi\delta^1 J_{d,X} + 2I_z^d X_z \sin 2\pi\delta^1 J_{d,X} \\ I_y^d &\longrightarrow I_y^d \\ 2I_x^d X_z &\longrightarrow -2I_x^d X_z \cos 2\pi\delta^1 J_{d,X} - I_z^d \sin 2\pi\delta^1 J_{d,X} \\ 2I_y^d X_z &\longrightarrow -2I_y^d X_z \end{aligned}$$

for proton transverse operators and

$$\begin{aligned} X_x &\longrightarrow X_x \cos 2\pi\delta^1 J_{d,X} - 2I_y^d X_y \sin 2\pi\delta^1 J_{d,X} \\ X_y &\longrightarrow -X_y \cos 2\pi\delta^1 J_{d,X} - 2I_y^d X_x \sin 2\pi\delta^1 J_{d,X} \\ 2I_z^d X_x &\longrightarrow 2I_z^d X_x \\ 2I_z^d X_y &\longrightarrow -2I_z^d X_y \end{aligned}$$

for the corresponding transverse operators of the heteronucleus. The magnetization of every other operator is scaled by $\cos(2\pi\delta^1 J_{d,X})$, resulting in an average loss of $0.5^*(1 - \cos(2\pi\delta^1 J_{d,X}))$ due to incomplete transfer during the BIRD^{d,X} filter.

To examine the influence of homonuclear and long-range heteronuclear couplings, we assume a perfectly matched delay δ , leading to $\cos(2\pi\delta^1 J_{d,X}) = -1$ and $\sin(2\pi\delta^1 J_{d,X}) = 0$. The transfers are then

$$\begin{aligned} I_x^d &\longrightarrow -I_x^d \cos 2\pi\delta^n J_{d,r} + 2I_z^d I_y^r \sin 2\pi\delta^n J_{d,r} \\ I_y^d &\longrightarrow I_y^d \\ 2I_x^d X_z &\longrightarrow 2I_x^d X_z \cos 2\pi\delta^n J_{d,r} + 4I_z^d I_y^r X_z \sin 2\pi\delta^n J_{d,r} \\ 2I_y^d X_z &\longrightarrow -2I_y^d X_z \end{aligned}$$

and

$$\begin{aligned} X_x &\longrightarrow -X_x \cos 2\pi\delta^1 J_{r,X} + 2I_y^r X_y \sin 2\pi\delta^1 J_{r,X} \\ X_y &\longrightarrow X_y \cos 2\pi\delta^1 J_{r,X} + 2I_y^r X_x \sin 2\pi\delta^1 J_{r,X} \\ 2I_z^d X_x &\longrightarrow 2I_z^d X_x \cos 2\pi\delta^1 J_{r,X} \cos 2\pi\delta^n J_{d,r} \\ &\quad -4I_z^d I_y^r X_y \sin 2\pi\delta^1 J_{r,X} \cos 2\pi\delta^n J_{d,r} \\ &\quad +4I_z^d I_y^r X_x \cos 2\pi\delta^1 J_{r,X} \sin 2\pi\delta^n J_{d,r} \\ &\quad -2I_z^d X_y \sin 2\pi\delta^1 J_{r,X} \sin 2\pi\delta^n J_{d,r} \\ 2I_z^d X_y &\longrightarrow -2I_z^d X_y \cos 2\pi\delta^1 J_{r,X} \cos 2\pi\delta^n J_{d,r} \\ &\quad -4I_z^d I_y^r X_x \sin 2\pi\delta^1 J_{r,X} \cos 2\pi\delta^n J_{d,r} \\ &\quad -4I_z^d I_y^r X_y \cos 2\pi\delta^1 J_{r,X} \sin 2\pi\delta^n J_{d,r} \\ &\quad -2I_z^d X_x \sin 2\pi\delta^1 J_{r,X} \sin 2\pi\delta^n J_{d,r} \end{aligned}$$

As with the direct one-bond coupling, every other transverse component is scaled by the homonuclear coupling $\cos(2\pi\delta^1 J_{d,r})$, causing an average loss of magnetization of $0.5^*(1 - \cos(2\pi\delta^1 J_{d,r}))$. Heteronuclear long-range couplings, instead, do not affect proton

transverse operators, but reduce all transverse operators on the heteronucleus according to $(1 - \cos(2\pi\delta^1 J_{r,X}))$.

References

- Bax A (2003) Weak alignment offers new NMR opportunities to study protein structure and dynamics. *Protein Science* 12:1–16
- Bax A, Tjandra N (1997) High-resolution heteronuclear NMR of human ubiquitin in an aqueous liquid crystalline medium. *J Biomol NMR* 10:289–292
- Bendiak B (2002) Sensitive through-space dipolar correlations between nuclei of small organic molecules by partial alignment in a deuterated liquid solvent. *J Am Chem Soc* 124:14862–14863
- Bruschweiler R, Zhang FL (2004) Covariance nuclear magnetic resonance spectroscopy. *J Chem Phys* 120:5253–5260
- Brutscher B, Boisbouvier J, Pardi A, Marion D, Simorre JP (1998) Improved sensitivity and resolution in H-1-C-13 NMR experiments of RNA. *J Am Chem Soc* 120:11845–11851
- de Alba E, Weiler S, Tjandra N (2003) Solution structure of human Saposin C: pH-dependent interaction with phospholipid vesicles. *Biochemistry* 42:14729–14740
- Delaglio F, Grzesiek S, Vuister GW, Zhu G, Pfeifer J, Bax A (1995) NMRpipe – a multidimensional spectral processing system based on unix pipes. *J Biomol NMR* 6:277–293
- Fehér K, Berger S, Kövér KE (2003) Accurate determination of small one-bond heteronuclear residual dipolar couplings by F1 coupled HSQC modified with a G-BIRD^r module. *J Magn Reson* 163:340–346
- Freedberg DI (2002) An alternative method for pucker determination in carbohydrates from residual dipolar couplings: A solution NMR study of the fructofuranosyl ring of sucrose. *J Am Chem Soc* 124:2358–2362
- Freeman R, Kupce E (2003) New methods for fast multidimensional NMR. *J Biomol NMR* 27:101–113
- Freudenberger JC, Knör S, Kobzar K, Heckmann D, Paululat T, Kessler H, Luy B (2005) Stretched poly(vinyl acetate) gels as NMR alignment media for the measurement of residual dipolar couplings in polar organic solvents. *Angew Chem Int Ed* 44:423–426
- Freudenberger JC, Spittler P, Bauer R, Kessler H, Luy B (2004) Stretched poly(dimethylsiloxane) gels as NMR alignment media for apolar and weakly polar organic solvents: An ideal tool for measuring RDCs at low molecular concentrations. *J Am Chem Soc* 126:14690–14691
- Goddard TD, Kneller DG San Francisco, University of California
- Haberz P, Farjon J, Griesinger C (2005) A DMSO-compatible orienting medium: Towards the investigation of the stereochemistry of natural products. *Angew Chem Int Ed* 44:427–429
- Hansen MR, Mueller L, Pardi A (1998) Tunable alignment of macromolecules by filamentous phage yields dipolar coupling interactions. *Nat Struct Biol* 5:1065–1074
- John M, Wendeler M, Heller M, Sandhoff K, Kessler H (2006) Characterization of human saposins by NMR spectroscopy. *Biochemistry* 45:5206–5216
- Jung YS, Sharma M, Zweckstetter M (2004) Simultaneous assignment and structure determination of protein

- backbones by using NMR dipolar couplings. *Angew Chem Int Ed* 43:3479–3481
- Jung YS, Zweckstetter M (2004a) Backbone assignment of proteins with known structure using residual dipolar couplings. *J Biomol NMR* 30:25–35
- Jung YS, Zweckstetter M (2004b) Mars – robust automatic backbone assignment of proteins. *J Biomol NMR* 30:11–23
- Kessler H (1982) Peptide conformations 19 Conformation and biological activity of cyclic peptides. *Angewandte Chemie-International Edition in English* 21:512–523
- Kim S, Szyperski T (2003) GFT NMR, a new approach to rapidly obtain precise high-dimensional NMR spectral information. *J Am Chem Soc* 125:1385–1393
- Klages J, Neubauer C, Coles M, Kessler H, Luy B (2005) Structure refinement of Cyclosporin A in chloroform by using RDCs measured in a stretched PDMS-gel. *ChemBioChem* 6:1672–1678
- Kneller DG, Kuntz ID (1993) *J Cell Biochem Suppl* 17 C:254
- Kobzar K, Kessler H, Luy B (2005) Stretched gelatin gels as chiral alignment media for the discrimination of enantiomers by NMR spectroscopy. *Angew Chem Int Ed* 44:3145–3147
- Koskela H, Kilpelainen I, Heikkinen S (2004) CAGEBIRD: improving the GBIRD filter with a CPMG sequence. *J Magn Reson* 170:121–126
- Kövér KE, Batta G (2004) More line narrowing in TROSY by decoupling of long-range couplings: shift correlation and $^1\text{J}_{\text{NC}}$ coupling constant measurements. *J Magn Reson* 170:184–190
- Kövér KE, Forgó P (2004) J-modulated ADEQUATE (JM-ADEQUATE) experiment for accurate measurement of carbon-carbon coupling constants. *J Magn Reson* 166:47–52
- Luy B, Barchi JJ, Marino JP (2001) S3E-E.COSY methods for the measurement of F-19 associated scalar and dipolar coupling constants. *J Magn Reson* 152:179–184
- Luy B, Marino JP (2001a) Measurement and application of H-1-F-19 dipolar couplings in the structure determination of 2'-fluorolabeled RNA. *J Biomol NMR* 20:39–47
- Luy B, Marino JP (2001b) H-1-P-31 CPMG-correlated experiments for the assignment of nucleic acids. *J Am Chem Soc* 123:11306–11307
- Luy B, Kobzar K, Kessler H (2004) An easy and scalable method for the partial alignment of organic molecules for measuring residual dipolar couplings. *Angew Chem Int Ed* 43:1092–1094
- Luy B, Kobzar K, Knör S, Furrer J, Heckmann D, Kessler H (2005) Orientational properties of stretched polystyrene gels in organic solvents and the suppression of their residual H-1 NMR signals. *J Am Chem Soc* 127:6459–6465
- Luy B, Marino JP (2003) JE-TROSY: combined J- and TROSY-spectroscopy for the measurement of one-bond couplings in macromolecules. *J Magn Reson* 163:92–98
- Mandelshtam VA, Taylor HS, Shaka AJ (1998) Application of the filter diagonalization method to one- and two-dimensional NMR spectra. *J Magn Reson* 133:304–312
- Martin-Pastor M, Bush CA (2001) Refined structure of a flexible heptasaccharide using H-1-C-13 and H-1-H-1 NMR residual dipolar couplings in concert with NOE and long range scalar coupling constants. *J Biomol NMR* 19:125–139
- Meissner A, Duus JO, Sørensen OW (1997a) Integration of spin-state-selective excitation into 2D NMR correlation experiments with heteronuclear ZQ/2Q pi rotations for $^1\text{J}_{\text{XH}}$ -resolved E.COSY-type measurement of heteronuclear coupling constants in proteins. *J Biomol NMR* 10:89–94
- Meissner A, Duus JO, Sørensen OW (1997b) Spin-state-selective excitation. Application for E.COSY-type measurement of J_{HH} coupling constants. *J Magn Reson* 128:92–97
- Mierke DF, Kurz M, Kessler H (1994) Peptide flexibility and calculations of an ensemble of molecules. *J Am Chem Soc* 116:1042–1049
- Mori S, Abeygunawardana C, Johnson MO, Vanzijl PCM (1995) Improved sensitivity of HSQC spectra of exchanging protons at short interscan delays using a new fast HSQC (FHSQC) detection scheme that avoids water saturation. *J Magn Reson B* 108:94–98
- Ottiger M, Delaglio F, Bax A (1998a) Measurement of J and dipolar couplings from simplified two-dimensional NMR spectra. *J Magn Reson* 131:373–378
- Ottiger M, Delaglio F, Marquardt JL, Tjandra N, Bax A (1998b) Measurement of dipolar couplings for methylene and methyl sites in weakly oriented macromolecules and their use in structure determination. *J Magn Reson* 134:365–369
- Permi P (2002) A spin-state-selective experiment for measuring heteronuclear one-bond and homonuclear two-bond couplings from an HSQC-type spectrum. *J Biomol NMR* 22:27–35
- Pham TN, Liptaj T, Bromek K, Uhrin D (2002) Measurement of small one-bond proton-carbon residual dipolar coupling constants in partially oriented C-13 natural abundance oligosaccharide samples: Analysis of heteronuclear $^1\text{J}_{\text{CH}}$ -modulated spectra with the BIRD inversion pulse. *J Magn Reson* 157:200–209
- Piotto M, Saudek V, Sklenar V (1992) Gradient-tailored excitation for single-quantum NMR-spectroscopy of aqueous solutions. *J Biomol NMR* 2:661–665
- Prestegard JH (1998) New techniques in structural NMR – anisotropic interactions. *Nat Struct Biol* 5:517–522
- Shaka AJ, Barker PB, Freeman R (1985) Computer-optimized decoupling scheme for wideband applications and low-level operation. *J Magn Reson* 64:547–552
- Simon B, Sattler M (2002) De Novo structure determination from residual dipolar couplings by NMR spectroscopy. *Angew Chem Int Ed* 41:437–440
- Sklenar V, Piotto M, Leppik R, Saudek V (1993) Gradient-tailored water suppression for H-1-N-15 HSQC experiments optimized to retain full sensitivity. *J Magn Reson A* 102:241–245
- Thiele CM (2004) Simultaneous assignment of all diastereotopic protons in strychnine using RDCs: PELG as alignment medium for organic molecules. *J Org Chem* 69:7408–7413
- Thiele CM (2005) Scaling the alignment of small organic molecules in substituted polyglutamates by variable-angle sample spinning. *Angew Chem Int Ed* 44:2787–2790
- Thiele CM, Berger S (2003) Probing the diastereotopicity of methylene protons in strychnine using residual dipolar couplings. *Org Lett* 5:705–708
- Tjandra N, Bax A (1997a) Direct measurement of distances and angles in biomolecules by NMR in a dilute liquid crystalline medium. *Science* 278:1111–1114
- Tjandra N, Bax A (1997b) Measurement of dipolar contributions to $^1\text{J}_{\text{CH}}$ splittings from magnetic-field dependence of J modulation in two-dimensional NMR spectra. *J Magn Reson* 124:512–515
- Tjandra N, Omichinski JG, Gronenborn AM, Clore GM, Bax A (1997) Use of dipolar H-1-N-15 and H-1-C-13 couplings in the structure determination of magnetically oriented macromolecules in solution. *Nat Struct Biol* 4:732–738
- Tolman JR, Prestegard JH (1996a) Measurement of amide N-15-H-1 one-bond couplings in proteins using accordion

- heteronuclear-shift-correlation experiments. *J Magn Reson B* 112:269–274
- Tolman JR, Prestegard JH (1996b) A quantitative J-correlation experiment for the accurate measurement of one-bond amide N-15-H-1 couplings in proteins. *J Magn Reson B* 112:245–252
- Uhrin D, Liptaj T, Kövér KE (1993) Modified BIRD pulses and design of heteronuclear pulse sequences. *J Magn Reson A* 101:41–46
- Verdier L, Sakhaii P, Zweckstetter M, Griesinger C (2003) Measurement of long range H,C couplings in natural products in orienting media: a tool for structure elucidation of natural products. *J Magn Reson* 163:353–359
- Wendeler M, Hoernschemeyer J, John M, Werth N, Schoeniger M, Lemm T, Hartmann R, Kessler H, Sandhoff K (2004) Expression of the GM2-activator protein in the methylotrophic yeast *Pichia pastoris*, purification, isotopic labeling, and biophysical characterization. *Protein Expression and Purification* 34:147–157
- Yan JL, Delaglio F, Kaerner A, Kline AD, Mo HP, Shapiro MJ, Smitka TA, Stephenson GA, Zartler ER (2004) Complete relative stereochemistry of multiple stereocenters using only residual dipolar couplings. *J Am Chem Soc* 126:5008–5017
- Yan JL, Kline AD, Mo HP, Shapiro MJ, Zartler ER (2003) A novel method for the determination of stereochemistry in six-membered chairlike rings using residual dipolar couplings. *J Org Chem* 68:1786–1795
- Yang DW, Tolman JR, Goto NK, Kay LE (1998) An HNCQ-based pulse scheme for the measurement of C-13(alpha)-H-1(alpha) one-bond dipolar couplings in N-15, C-13 labeled proteins. *J Biomol NMR* 12:325–332